

ChemComm

Accepted Manuscript



This is an *Accepted Manuscript*, which has been through the Royal Society of Chemistry peer review process and has been accepted for publication.

Accepted Manuscripts are published online shortly after acceptance, before technical editing, formatting and proof reading. Using this free service, authors can make their results available to the community, in citable form, before we publish the edited article. We will replace this *Accepted Manuscript* with the edited and formatted *Advance Article* as soon as it is available.

You can find more information about *Accepted Manuscripts* in the [Information for Authors](#).

Please note that technical editing may introduce minor changes to the text and/or graphics, which may alter content. The journal's standard [Terms & Conditions](#) and the [Ethical guidelines](#) still apply. In no event shall the Royal Society of Chemistry be held responsible for any errors or omissions in this *Accepted Manuscript* or any consequences arising from the use of any information it contains.

COMMUNICATION

Self-assembling a neutral platinum(II) complex into highly emitting microcrystalline fibers through metallophilic interactions†

Cite this: DOI: 10.1039/x0xx00000x

Received 00th January 2012,
Accepted 00th January 2012

DOI: 10.1039/x0xx00000x

www.rsc.org/

Matteo Mauro,^{*,a,b} Alessandro Aliprandi,^a Cristina Cebrián,^{a,c} Di Wang,^d Christian Kübel,^d and Luisa De Cola^{*,a,d}

The solvent-assisted self-assembly of blue-emitting neutral platinum(II) complexes into micrometer-long and highly crystalline fibers has been achieved. The aggregates show highly efficient (quantum yield up to 74%) polarized yellow-orange light emission, as consequence of their high degree of supramolecular order imparted by weak non-covalent intermolecular (metal...metal and π - π) interactions.

Supramolecular organometallic nanostructures have attracted a great deal of attention in the last few years because of the possibility to fabricate functional materials with superior properties compared to the bulk. In particular, square-planar Pt(II) and Pd(II) complexes with protruding filled d_{z^2} orbitals have been known for a long time to show a high tendency towards stacking, through weak non-covalent metal...metal and/or π - π ligand-ligand interactions.¹ By means of bottom-up approach, it has been shown that luminescent Pt(II) complexes are able to form either homo-² or hetero-metallic³ supramolecular architectures as liquid crystals,⁴ nanowires,⁵ nanotubes,⁶ nanosheets,⁷ and metallogelators,^{8,9a} with very appealing (electro)optical,⁹⁻¹¹ sensing,¹² and semiconducting properties.^{7,13}

To date, metal complexes forming long-range ordered soft structures showing polarized light emission and photoluminescence quantum yield (PLQY) exceeding 0.5 are very rare and typically require aid of orienting scaffolds and special techniques.^{9b,14} This is despite the great potential applications that such self-assembled functional architectures might have in optoelectronic devices such as organic light emitting diodes (OLEDs),⁹ field effect transistors (FETs),^{7,13} and organic light-emitting FETs (OLEFETs).¹¹ Noteworthy, linearly polarized materials with uniaxial molecular orientation find great application for improving light extraction in such devices,^{9b} and as active materials in 3D OLED displays.¹⁴

In this communication, we report on the synthesis and characterization of a neutral Pt(II) complex, namely **Pt-CF₃tz-pyC₅**, containing a formally dianionic N-donor tridentate chromophoric ligand. Such complex, because of a square-planar geometry, displays great tendency to aggregate in bright polarized-light emitting fibers.

The compound belongs to the class of highly luminescent Pt(II) complexes recently reported by our group,¹⁵ bearing N⁻N⁻N azoles-based ligands and the chemical structure depicted in Fig. 1. The one-

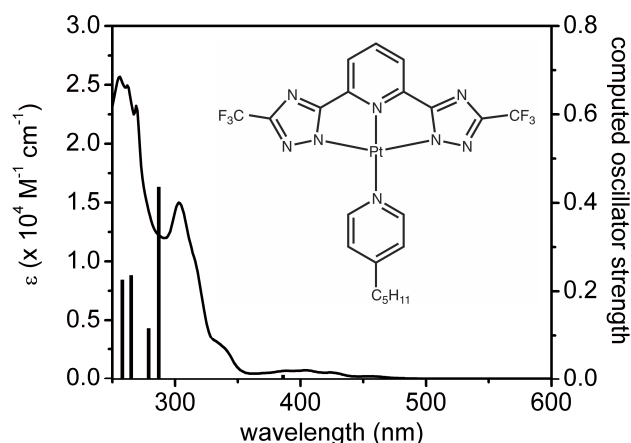


Fig. 1. Absorption spectrum obtained for the complex **Pt-CF₃tz-pyC₅** (inset) in CHCl₃ at room temperature and TD-DFT vertical transitions with the corresponding computed oscillator strength.

pot synthetic procedure employs PtCl₂(DMSO)₂ (DMSO = dimethylsulfoxide) as the Pt(II) precursor, diisopropylethylamine as the base, 4-aminopyridine as the ancillary ligand and 2,6-bis(3-(trifluoromethyl)-1H-1,2,4-triazol-5-yl)pyridine (**pyC₅-CF₃-tzH₂**), as the tridentate ligand in a 3:1 2-methoxyethanol:H₂O solvent mixture at 83°C. The final pure compound was obtained by column chromatography and fully characterized by ¹H, ¹³C and ¹⁹F NMR and high-resolution mass spectrometry. Interestingly, the complex is extremely soluble in halogenated solvents and ethers. The experimental details are given in the Electronic Supplementary Information (ESI).

Geometrical structure optimization by means of density functional theory (DFT) has been performed for the compound **Pt-**

CF₃tz-pyC₅ in its electronic ground state (S_0). In its lowest-energy geometry, the complex adopts a distorted square-planar arrangement around the metal atom with C_s point group symmetry. The computed bond distances are 2.027, 1.998 and 2.052 Å for Pt–N(1), Pt–N(4) and Pt–N(5), respectively, which nicely agree with other similar Pt(II) complexes.¹⁵ The atoms labelling and a more complete list of geometrical parameters can be found in Fig. S1 and Table S1 of the ESI, respectively. In order to gain insights into the frontier orbitals and the redox processes of the complex **Pt-CF₃tz-pyC₅**, cyclic voltammetry (CV) measurements were performed in CH₂Cl₂ as the solvent and tetrabutylammonium hexafluorophosphate (TBAPF₆) as the supporting electrolyte (see ESI for further details and Fig. S2). The cyclic voltammogram displays a reversible reduction process at –1.83 V (*vs* Fc⁺/Fc), which is mainly located on the pyridilic moiety of the tridentate ligand, where the lowest unoccupied molecular orbitals, i.e. LUMO, is located. Such assignment is also supported by the frontier orbital analysis carried out on the S_0 DFT-optimized geometry. Further computational results are given in Table S2, and the isodensity surface plots are depicted in Fig. S3 of the ESI. No oxidation process is visible in the employed observation window.

As shown in Fig. 1, in dilute (concentration 5×10^{-5} M) CHCl₃ solution at room temperature, the absorption spectrum displays intense bands in the UV region ($\lambda = 254$ nm, $\epsilon = 2.3 \times 10^4$ M⁻¹ cm⁻¹; $\lambda = 302$ nm, $\epsilon = 1.5 \times 10^4$ M⁻¹ cm⁻¹; $\lambda = 337$ nm, $\epsilon = 2.6 \times 10^3$ M⁻¹ cm⁻¹). These transitions are mainly attributed to the intraligand (¹IL) and metal-perturbed interligand charge transfer (¹ILCT) states.

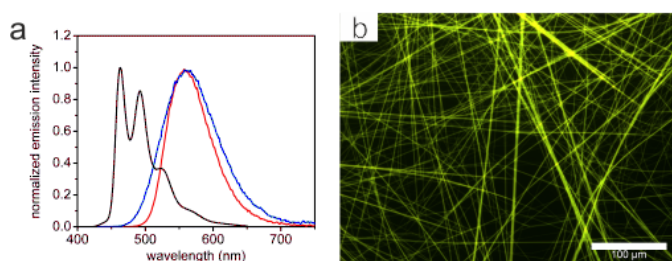


Fig. 2. a) Emission spectra obtained for the complex **Pt-CF₃tz-pyC₅** in CHCl₃ (black trace) at concentration of 5×10^{-5} M, self-assembled fibers obtained from acetone at concentration of 4 mg mL⁻¹ (red trace), fibers obtained from CH₂Cl₂ at concentration of 4 mg mL⁻¹ (blue trace), upon excitation at $\lambda_{exc} = 300$ nm. b) fluorescence microscopy image of the fibers obtained from acetone under irradiation at $\lambda = 400$ –440 nm. Scale bar = 100 μm.

At lower energy a broad band in the region 350–450 nm (ϵ ca. 0.7×10^3 M⁻¹ cm⁻¹) is assigned to the HOMO → LUMO ($f = 0.01$, 3.211 eV, 386 nm), and ascribed to the admixture of spin-allowed metal-to-ligand charge transfer (¹MLCT) and intraligand (¹IL) transitions. These assignments are further corroborated by the similarity with already reported Pt(II) complexes,¹⁵ and by time-dependent DFT (TD-DFT) calculation in CHCl₃ at PBE1PBE and SDD + 6-31g(d,p) level. A more complete list of electronic transitions computed both in vacuum and CHCl₃ solvent is given in Table S3 of the ESI.

Fig. 2a shows the emission spectrum in degassed CHCl₃ solution of the complex. A structured blue luminescence is observed, peaking at $\lambda_{em} = 463, 493, 525$ and 570 (shoulder) nm, with vibronical

progression of 1236–1504 cm⁻¹ attributable to the tridentate intraligand vibrational modes. Such moderate (PLQY = 2%) luminescence is characterized by a very fast radiative decay, with a multi-exponential excited-state lifetime, being $\tau_1 = 10$ ns (48%) and $\tau_2 = 309$ ns (52%). The bi-exponential decay is due to the equilibrium between the emissive ³MLCT/³LC and a thermally populated non-radiative state. Hence, such emission can be attributed to the $T_1 \rightarrow S_0$ radiative transition with mainly metal-perturbed ³LC character, and the highest energy peak observed at 298 K (463 nm, 2.68 eV) agrees with the theoretical $S_0 \rightarrow T_1$ (HOMO → LUMO) vertical excitation process computed at 432 (2.87 eV) nm in CHCl₃.

Interestingly, the complex exhibits very different photophysical behaviour in the solid state. In the attempt to crystallize the compound to obtain good quality single-crystal suitable for X-ray analysis, we have isolated yellow bright emissive microcrystalline fibers. The luminescent fibers, Fig. 2b, can be obtained when an acetone solution of the **Pt-CF₃tz-pyC₅** complex is slowly concentrated by evaporation (see ESI for details). Upon photo-irradiation with UV light, such discrete fibers showed intense and featureless emission centred at $\lambda_{em,max} = 559$ nm with PLQY as high as 0.74 (see Fig. 2a). Such great increase of the emission quantum yield is accompanied by a concomitant prolongation of the mono-exponential decay of the excited-state ($\tau = 355$ ns). Furthermore, the employed solvent plays also an important role in the photophysical properties of the self-assembled structures. Indeed, CH₂Cl₂ solution at concentration of 4 mg mL⁻¹ yields fibers with slightly broader emission spectra peaking at $\lambda_{em,max} = 563$ and with PLQY of 0.58.

The sizeable bathochromic shift, the featureless emission profile, and the high emission quantum yield are already strong indications that the emissive state of the fibers is different from the luminescent level of the complex in solution. Furthermore, the outcome is not a merely rigidochromic effect since the nature of the emission is different.

It is well known that the square planar geometry of the compound can favour aggregates formation leading to Pt...Pt interactions, through the d_z^2 orbitals of the metals that rise in energy and become the HOMO orbitals of the assemblies. As a consequence the nature of the lowest electronic transitions can change from ligand centered to metal-metal ligand charge transfer, MMLCT. For our system the strong coupling between the two platinum units is observed by the appearance of a lower energy band in the excitation spectrum of the fiber ($\lambda = 501$ nm), as displayed in Fig. S4 (ESI). The transition involved has been ascribed as ¹MMLCT. Excitation in this band, as well as in any other absorption leads to the yellow emission attributed to the corresponding ³MMLCT. Furthermore, such solvophobic metallophilic interactions are accounted to play a major role into the nanoscale organization and molecular propagation for the self-assembly of the **Pt-CF₃tz-pyC₅** complex. As a result of this long-range order, light emission perpendicularly polarized with respect to the fiber growth axis is unambiguously observed, as shown in Fig. S5 and Movie S1 of the ESI.

Morphological and structural characterization of these Pt(II) aggregates has been performed by both scanning (SEM) and transmission electron microscopy (TEM) techniques, Fig. 3, as well as small-angle X-ray scattering, (SAXS). As shown in the SEM images, the sample of the emissive soft-structures prepared from

acetone (concentration 4 mg mL^{-1}) is comprised of hundreds of micrometres long one-dimensional (1D) fibers. On the other hand, samples prepared from CH_2Cl_2 at similar concentration gave a more tri-dimensional (3D) interconnected network of fibers (data not shown). In both cases, such fibrous nanostructures seem to be the result of a self-assembly process of thinner nanostructures such as

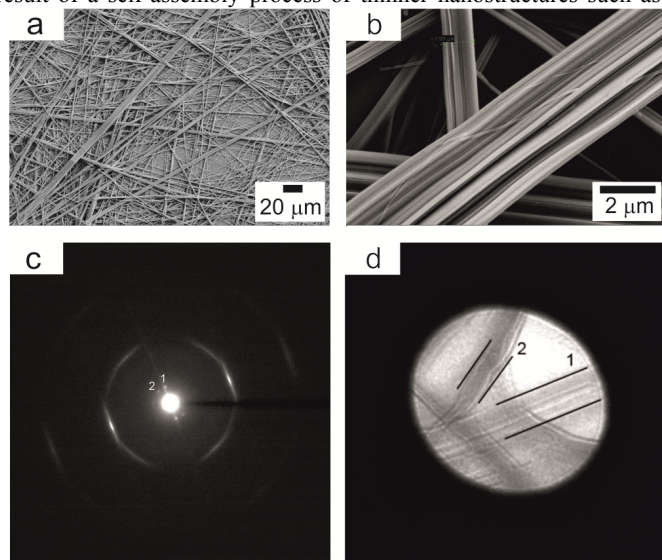


Fig. 3. SEM images taken on a sample of fibers of complex $\text{Pt-CF}_3\text{tz-pyC}_5$ obtained from acetone at concentration of 4 mg mL^{-1} (a) and zoom-in image (b); c) SAED pattern from a few fibres as shown in the corresponding shadow image (d).

nanofibrils. SEM analysis, however, could not give us any information on the packing and crystallinity of the assembly.

Additionally, SAXS/WAXS experiments were performed on fibers prepared by drop-casting a 4 mg mL^{-1} acetone solution, which is the same experimental condition to obtain the fibers investigated by means of spectroscopic techniques. The scattering pattern, which displays sharp peaks, confirmed the high degree of long-range order within the self-assembled structures, as shown in Fig. S6 of the ESI. Noteworthy, it is possible to detect a scattering peak at 3.28 \AA that can be most likely ascribed to the distance corresponding to $d_z^2\pi \cdots d_z^2\pi$ intermolecular interaction leading to the strong bathochromic shift of the emission into the self-assembled fibers (see Fig. S7 of the ESI).

Finally, to explore the crystal structure of the Pt(II) aggregates prepared from acetone, selected area electron diffraction (SAED) patterns were acquired corresponding to a local region with a few fibers present. In order to avoid damage of the crystal structure as a consequence of the electron beam, very low dose rate was employed for the analysis (see ESI for details). The morphology and orientation of the fibers contributing to electron diffraction were obtained looking at the shadow image in the central disk of a largely defocused diffraction pattern. Fig. 3c–d show a representative diffraction pattern and the corresponding shadow image. In the diffraction pattern, two pairs of spots close to the central beam correspond to a lattice period of 1.33 nm . The diffraction vectors are perpendicular to the two groups of fibers numbered in the shadow image, respectively. This indicates a periodic self-assembly of the Pt complex chains perpendicular to the fiber long axis. In addition,

strongly streaked diffraction spots corresponding to a lattice period of 3.53 \AA were observed parallel to the molecular propagation vector. This lattice period is different to that obtained by X-ray scattering analysis and is most likely due to different sample preparation required for the TEM analysis (lower concentration and fast evaporation rate). However, this periodicity can be attributed to the long-range order of the complex along the fiber axis, while the streaking of these spots perpendicular to such axis indicates a shift disorder of the stacked complexes along the fibre long axis.

Conclusions

The synthesis and characterization of a novel blue emitting platinum(II) complexes based on $\text{N}^{\wedge}\text{N}^{\wedge}\text{N}$ chromophoric ligand is reported. The compound shows a remarkable tendency to spontaneously assemble into highly ordered structures, such as fibers, through metal \cdots metal and π - π interactions. The assemblies efficiently emit polarized yellow light, as shown by fluorescent microscopy, with the remarkably high PLQY value of 74%, which might find application in polarized light-emitting devices and 3D OLED displays. To gain insight into the structural properties of the self-assembled structures SAED and SAXS/WAXS experiments were performed, which displayed an intermolecular distance of 3.28 \AA attributable to the $d_z^2\pi \cdots d_z^2\pi$ interactions along the growth axis of the fibers.

The authors kindly acknowledge Dr. S. Kehr for SEM images, and Dr. E. A. Prasetyanto for SAXS/WAXS measurements, and the LabEx “Chimie des Systèmes Complexes”. L.D.C. is grateful to the Région Alsace and the Communauté Urbaine de Strasbourg, the Gutenberg Excellence Chair (2011–2012) and to AXA Research funds. KIT is gratefully acknowledged for TEM availability in the frame of the Karlsruhe Nano Micro Facility (KNMF) project “Self-assembly for and in confined space”.

Notes and references

^a ISIS & icFRC, Université de Strasbourg & CNRS, 8 rue Gaspard Monge, 67000 Strasbourg, France Fax: +33 (0) 3 6885 5242; Tel: +33 (0) 3 6885 5220; E-mail: mauro@unistra.fr, decola@unistra.fr.

^b University of Strasbourg Institute for Advanced Study (USIAS), 5 allée du Général Rouvillois, 67083 Strasbourg, France

^c Current address: Laboratoire de Structure et Réactivité des Systèmes Moléculaire Complexes (SRSMC) – UMR 7565, Institut de Chimie, Physique et Matériaux (ICPM), Université de Lorraine, 1 Boulevard Arago, 57070 Metz, France.

^d Institute of Nanotechnology and Karlsruhe Nano Micro Facility, Karlsruhe Institute of Technology (KIT), Hermann-von-Helmholtz Platz 1, 76344, Eggenstein-Leopoldshafen, Germany.

† Electronic Supplementary Information (ESI) available: Materials and methods, synthesis, photophysical, electron microscopies and computational details are given in the ESI. See DOI: 10.1039/c000000x/

- V. M. Miskowski, V. H. Houlding, *Coord. Chem. Rev.*, 1991, **111**, 145–152; D. M. Roundhill, H. B. Gray, C.-M. Che, *Acc. Chem. Res.*, 1989, **22**, 55–61; P. Pykkö *Chem. Rev.*, 1997, **97**, 597–636.

- 2 S. Y. L. Leung, W. H. Lam, V. W.-W. Yam, *Proc. Nat. Acad. Sci. USA*, 2013, **11**, 7986–7991.
- 3 X. Zhang, B. Cao, E. J. Valente, T. K. Hollis, *Organometallics*, 2013, **32**, 752–761; Y. Tanaka, K. M. C. Wong, V. W.-W. Yam, *Chem. Sci.*, 2012, **3**, 1185–1191.
- 4 V. N. Kozhevnikov, B. Donnio, D. W. Bruce, *Angew. Chem. Int. Ed.*, 2008, **47**, 6286–6289.
- 5 Y. Sun, K. Ye, H. Zhang, J. Zhang, L. Zhao, B. Li, G. Yang, B. Yang, Y. Wang, S. W. Lai, C.-M. Che, *Angew. Chem. Int. Ed.*, 2006, **118**, 5738–5741.
- 6 W. Zhang, W. Jin, T. Fukushima, N. Ishii, T. Aida, *Angew. Chem. Int. Ed.*, 2009, **48**, 4747–4750.
- 7 Y. Che, K. Li, W. Lu, S. S.-Y. Chui, C.-W. Ma, C.-M. Che, *Angew. Chem. Int. Ed.*, 2009, **48**, 9009–9913.
- 8 Y. Li, E. S. H. Lam, A. Y. Y. Tam, K. M. C. Wong, W. H. Lam, L. Wu, V. W.-W. Yam, *Chem. Eur. J.*, 2013, **19**, 9987–9994.
- 9 a) C. A. Strassert, C.-H. Chien, M. D. Galvez Lopez, D. Kourkoulos, D. Hertel, K. Meerholz, L. De Cola, *Angew. Chem. Int. Ed.*, 2011, **50**, 946–950; b) M. Taneda, T. Yasuda, C. Adachi, *Appl. Phys. Express*, 2011, **4**, 071602–3.
- 10 S. Y. L. Leunga, V. W.-W. Yam, *Chem. Sci.*, 2013, **4**, 4228–4234.
- 11 M. Y. Yuen, V. A. L. Roy, W. L., S. C. F. Kui, G. S. M. Tong, M. H. So, S. S. Y. Chui, M. Muccini, J. Q. Ning, S. J. Xu, C.-M. Che, *Angew. Chem. Int. Ed.*, 2008, **47**, 9895–9899.
- 12 M. C. L. Yeunga, V. W.-W. Yam, *Chem. Sci.*, 2013, **4**, 2928–2935;
- 13 C. M. Che, C. F. Chow, M. Y. Yuen, V. A. L. Roy, W. Lu, Y. Chen, S. S. Y. Chui, N. Zhu, *Chem. Sci.*, 2011, **2**, 216–222.
- 14 M. Grell, D. D. C. Bradley, *Adv. Mater.*, 1999, **11**, 895–905.
- 15 a) C. Cebrián, M. Mauro, D. Kourkoulos, P. Mercandelli, D. Hertel, K. Meerholz, C. A. Strassert, L. De Cola, *Adv. Mater.*, 2013, **25**, 437–442; b) M. Mydlak, M. Mauro, F. Polo, M. Felicetti, J. Leonhardt, G. Diener, L. De Cola, C. A. Strassert, *Chem. Mater.*, 2011, **23**, 3659–3667.